Orbital Tracking and Decay Analysis of the Saturn I Flights

H. F. KURTZ JR.,* M. NAUMCHEFF,† AND A. R. MCNAIR‡
NASA George C. Marshall Space Flight Center, Huntsville, Ala.

FOUR Saturn vehicles have been two-stage vehicles that inserted their second stages and payloads (Fig. 1) into orbit. Two aspects of the Marshall Space Flight Center (MSFC) orbit determinations for three of these Saturn vehicles are discussed in this note: the successful skin tracking of the orbiting vehicles by a network of FPS-16 and FPQ-6 instrumentation radars and the accurate determination of the effective atmospheric drag. The skin tracking was feasible because of the size of the vehicle and the resultant relatively large radar cross-sectional area. Reported observed areas have varied between 10 and 40 m².

The radar network included FPS-16 stations at Hawaii, White Sands, Eglin Air Force Base, Bermuda, Cape Kennedy, Ascension, Pretoria, and Point Arguello and FPQ-6 or TPQ-18 stations at Patrick Air Force Base, Grand Turk, Antigua, and Carnarvon. Essentially the same network has been used on all of the Saturn flights. It is basically the NASA Manned Space Flight Network with Department of Defense participation, and it is controlled by Goddard Space Flight Center (GSFC), using a real time computing complex. The network effectively sees about five consecutive orbital revolutions per day (3 min pass per station) followed by about ten nonvisible revolutions.

The initial skin-track attempts after the launch of SA-5 were disappointing; except for two poor quality tracks on the second day, no radars successfully acquired automatic track during the first week in orbit. However, after a few weeks of experience, the network was able to routinely track SA-5, obtaining valid data almost from horizon to horizon. The same network was able to skin track with great success the first Gemini-Titan (GT-1) orbit in April 1964, the SA-6 orbit in May 1964, and the SA-7 orbit in September 1964. The latter three flights each remained in orbit less than five days and were successfully tracked (~20 station passes per day) from launch until their uncontrolled re-entry from orbit because of atmospheric decay.

The Patrick, Carnarvon, and Antigua FPQ-6 radars and the extended-range FPS-16 radars at Eglin and White Sands have been able to consistently skin track on all of the Saturn vehicles and obtain excellent data. In addition, the Hawaii and Bermuda FPS-16 radars and the Grand Turk TPQ-18 were committed for the first time on SA-7 and achieved good results. Successful track has been accomplished by the FPQ-6 radars at slant ranges out to 1500 km with no apparent degradation in performance from short to long ranges. FPS-16 tracking has generally not been obtained when the minimum slant range from satellite to station during the pass exceeds about 300 km. The maximum slant range tracked during such a pass is about 700 km.

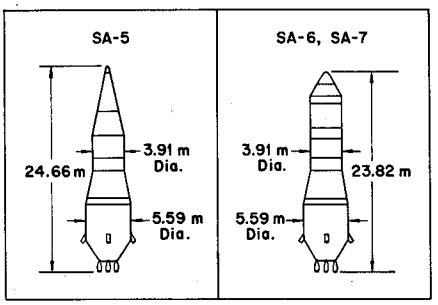

Fig. 1 Orbiting Saturn vehicles.

Table 1 SA-6 mean rms residuals

Tracking type	Data type: Azimuth, deg	Elevation, deg	Range
FPQ-6 skin track	0.021	0.029	23 m
FPQ-6 beacon track	0.009	0.028	4
FPS-16 skin track	0.023	0.059	37
FPS-16 beacon track	0.014	0.052	17

Tracking Analysis

The radar data have been used in a least-squares orbit determination to define the orbital ephemeris during the time of tracking; each orbit determination covers from two to four orbits on a given day. The orbit ephemeris thus defined is used to generate predicted azimuth, elevation, and range values for each station, and the residuals (differences) between observed and predicted values are determined. These residuals include random and systematic measuring errors, station location errors, and systematic errors in the orbit computation model. The residuals thus obtained on the Saturn vehicles are generally not distributed with zero men but indicate distinct systematic error trends that are presently undergoing analysis. Specific error types whose characteristics have been identified in the residuals include station timing errors, atmospheric refraction errors, and station location errors. It is believed the orbit computation model errors are small in comparison with station and measuring errors.

As a gross error measure, with no attempt to identify error components, the root-mean-square (rms) residuals for each data type from a given station on a given pass have been computed. Typical results are shown in Fig. 2, which shows the slant range residuals obtained during the SA-6 orbital lifetime. The data are plotted as a function of the minimum slant range during the pass which generally characterizes the length of the pass, the maximum elevation angle, and the relative distance. Beacon track was used during the first two orbits of SA-6 and skin track thereafter. Several points may be noted from this figure:

1) Only two of fourteen FPS-16 tracks were obtained at $R > 300$ km.

Table 2 Characteristic vehicle parameters and initial osculating orbital elements

	SA-5	SA-6	SA-7
Epoch, *UT*	16:35:41	17:17:35	16:33:14
Date	1/29/64	5/28/64	9/18/64
Semimajor axis, km	6889.85	6584.50	6585.32
Eccentricity × 10^4	369.49	42.83	40.92
Inclination, deg	31.46	31.78	31.75
Right ascension of ascending node, deg	177.02	304.48	44.87
Argument of perigee, deg	126.93	115.49	118.20
True anomaly, deg	8.09	20.25	17.71
Mass, kg	16,950	16,700	16,400
C_DA/M, m²/kg	0.0093	0.0104	0.0106
Lifetime, day	Predicted 800	Actual 3.3	Actual 3.8

Presented as Preprint 65-125 at the AIAA/NASA Flight Testing Conference, Huntsville, Ala., February 15–17, 1965; revision received April 5, 1965.

* Chief, Operations Studies Branch. Member AIAA.
† Chief, Orbit Determination Section.
‡ Chief, Mission Studies Section.

2) The scatter of the FPS-16 skin-track rms residuals is substantially greater than that of the FPS-16 beacon-track residuals; this statement is true to a much lesser degree for the FPQ-6 data.

3) The FPQ-6 residuals are essentially independent of range, except for an anomaly $R \simeq 350$ km.

The mean values of the rms residuals on SA-6 for azimuth, elevation, and range data are shown in Table 1. The over-all result of these data show that skin-track errors are quite comparable to beacon-track errors, and skin tracking affords quite precise orbital tracking.

Decay Analysis

Since the Saturn orbits have been well tracked, it has been possible to measure the effective drag on the orbiting vehicles quite well by including drag as an additional unknown that is solved for in a conventional orbit-determination program. The characteristic parameters of the orbit model are varied systematically in a numerical differential correction process until the values predicted by the model match in a least-square sense the values observed. The accuracy of the parameters derived in such an orbit determination obviously depends entirely upon the accuracy of the mathematical orbit model used and of the tracking data obtained.

The orbit model used in the MSFC orbit determination results to be presented included the second, third, and fourth zonal harmonics of the earth's gravitation field. It included an atmospheric drag model that used the 1959 Air Research and Development Command (ARDC) atmospheric density and assumed a constant ballistic factor for the satellite. The drag acceleration was calculated as $D = \frac{1}{2}K\ (C_DA/M)\ \rho\ V_E^2$, where C_D is the drag coefficient, A is the effective cross-sectional area, M is the satellite mass, ρ is the atmospheric density at the satellite, V_E is velocity relative to the surface of the earth, and K is a constant used nominally to compensate for variation of the actual current atmospheric density from the 1959 ARDC profile due to solar activity effects. When used as an unknown in an orbit determination, K may represent any constant-factor difference between the actual and predicted drag force.

The assumed values of the ballistic factors (C_DA/M) for SA-5, -6, and -7 are given in Table 2 along with other characteristic parameters of the vehicles. The vehicles were all assumed to have a random attitude in orbit. A drag coefficient C_D of 2.18 was assumed, and the effective cross-sectional area was computed as one-fourth of the total surface area of the vehicle

The radar tracking data of SA-6 and SA-7 were analyzed at MSFC with individual orbit determinations covering two to four consecutive revolutions. The initial osculating orbital elements obtained with these determinations were given in Table 2.

The data were also used in orbit determinations by the GSFC[1,2] and the Huntsville Research and Engineering

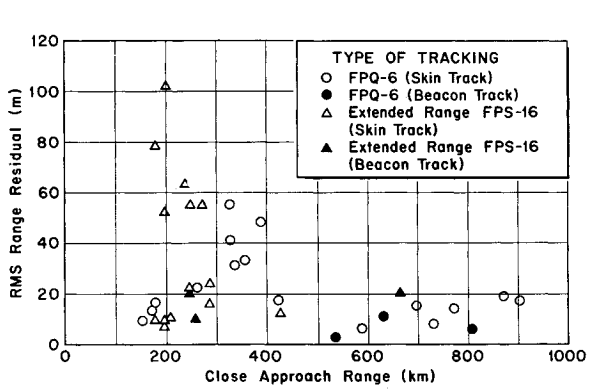

Fig. 2 Sa-6 gross rms range residuals.

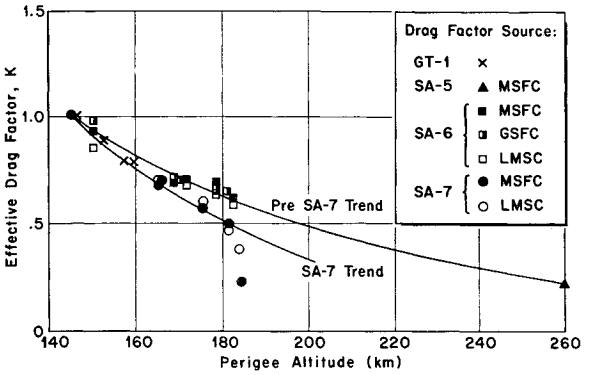

Fig. 3 Composite effective drag factors.

Center of the Lockheed Missiles & Space Co. (LMSC).[3,4] The GSFC method was quite similar to the MSFC method described earlier, whereas the LMSC orbit determinations were done by fitting orbital arcs of two days and assuming a second-degree polynominal as a drag-model correction factor. The three sets of results thus obtained are generally in good agreement, as shown in Fig. 3. The GSFC and LMSC results have been adjusted to assume the nominal ballistic factors given in Table 2. Each reference altitude used is the average between the minimum and maximum perigee altitudes experienced during the orbits of the given orbit determination. Figure 3 also shows drag values determined by radar skin track by GSFC for the GT-1[5] that had an initial perigee altitude of 160 km, an apogee altitude of 321 km, and re-entered after 4.2 days. The orbiting vehicle was similar in shape to the Saturn orbiting bodies but was approximately one-third the size. The values shown are adjusted from those given in Ref. 5 to be consistent with an MSFC computed ballistic factor for the GT-1 vehicle of 0.0089 m²/kg.

Also shown in Fig. 3 is one K (at 260 km) for the SA-5 vehicle; because of its higher altitude and smaller drag, no attempt has been made to derive K directly in an orbit determination as described for the other vehicles; the factor shown was derived from a comparison of the predicted and observed decay rate of the orbital semimajor axis, based on orbital elements determined over the past year by GSFC.

All of the results for SA-5, SA-6, and GT-1 exhibit a consistent trend that tends to validate (at least in a relative fashion) the assumed ballistic factors for these vehicles. The trend indicated is also consistent in shape, direction, and magnitude with the expected shift of current atmospheric density levels from the reference 1959 ARDC atmosphere. This shift reflects the current solar activity, which directly influences density at these altitudes. However, the SA-7 results, although demonstrating a similar trend in shape, direction, and general magnitude differ from the foregoing results by an amount much larger than the uncertainty of the drag measurements, which is estimated at $\pm 5\%$. The mean long-term solar activity level, as indicated by the 10.7 cm solar flux, was effectively constant over the period of all of the data presented. Investigations are continuing to determine the reasons for the difference, which may possibly be caused by a short-term atmospheric disturbance and small ballistic factor variations.

In summary, the drag determinations performed on the Saturn vehicles have provided valuable data concerning the drag characteristics of large vehicles in near-earth orbits and current atmospheric density levels. These data will result in increased confidence and reduced error bounds for decay prediction of similar future vehicles in the Apollo program.

References

[1] "Computing notes on the Saturn mission (SA-6)," Goddard Space Flight Center, X-554-64-166 (June 18, 1964).

[2] "Computing notes on the Saturn mission (SA-7)," Goddard Space Flight Center, X-550-64-269 (September 23, 1964).
[3] Richards, T. J. and Paul, L. K., Jr., "SA-6 post-flight orbit determination and decay analysis," Lockheed Missile & Space Co./Huntsville Research and Engineering Center A036606 (October 1964).
[4] Paul, L. K., Jr., "SA-7 post-flight orbit determination and decay analysis," Lockheed Missile & Space Co./Huntsville Research and Engineering Center A710290 (December 1964).
[5] "Computing notes on the first Gemini mission GT-1," Goddard Space Flight Center, X-554-64-102 (April 27, 1964).

Turbopump Transient Response Test Facility and Program

THOMAS C. SHUPERT* AND TERRY L. WARD†
Martin Company, Denver, Colo.

IN the Titan II missile, varying degrees of longitudinal vibrations were experienced. The intercontinental ballistic missile (ICBM) mission of the missile was not affected, but the longitudinal vibration phenomenon, better known as the Pogo phenomenon, was capable of affecting the manrated mission. Tests of individual components did not solve the problem, e.g., the natural frequency of the oxidizer feedline was found to be more than 1.5 times that of the Pogo phenomenon that occurred in flight. It was the coupling of the resonant frequencies of the missile structure and the fuel and oxidizer systems that produced the Pogo phenomenon. The final analysis of this problem was divided into the following two parts: the structure and the propulsion system. This note deals with the test program for the propulsion system, which was conducted in a "cold-flow" facility without a combustion chamber, since the combustion time lag was extremely short and was not considered to be a contributor to the Pogo phenomenon.

Test System

The test system (Fig. 1) was designed to duplicate the system parameters of the missile, to be capable of introducing pressure oscillations as specific points in the system, and to measure the outputs. Missile hardware was used where possible, but special equipment was required in certain areas because of the closed-loop system. The Titan II, stage I "battleship" tanks, installed in a 65-ft-high test stand, served as the basic facility. The tanks had the same internal configuration as missile tanks but had a wall thickness of approximately $\frac{3}{8}$ in. A separate pressurization system for each tank made it possible to hold pump suction pressures constant or to change them to new levels during a given test run.

The oxidizer (N_2O_4) feedline was specially designed, because only one turbopump subassembly was required, hence only one-half the nominal missile oxidizer flow rate was required. The 7-in.-diam line was designed to represent the same fluid inertance that one subassembly would experience. It had the same diameter/thickness ratio as the missile feedline in order to maintain the same fluid acoustic velocity. Twelve pressure transducers were installed along the line to measure wave propagation. The lowest of these was designated P_{os} pressure oxidizer suction. The pump suction line for the fuel (50 hydrazine-50 UDMH, called Aerozine 50) was connected directly to the fuel tank outlet.

Since turbomachinery introduced noise into the system, it was necessary to excite the system so that the desired transients possessed amplitudes in excess of the noise level but did not exceed the structural limitations of the system. The oxidizer and fuel lines were modified to incorporate pressure pulsers on the pump suction side. Each suction pulser (Fig. 2) consisted of a piston and bellows encased in a leakproof container driven by a varidrive motor. The amplitude of the pressure pulse was governed by the crank throw. The pressure pulse generated by the piston was directed into a torus (9.9 in. above the pump inlet flange) that was designed to induce uniform flow into the suction line. The suction pu ser design included adequate supports to prevent offset loading on the suction line, and bellows were installed above and below the torus to prevent lateral loads. The following equations were derived to describe the suction pulser piston displacement that would yield the desired pressure amplitude vs frequency:

$$P_1A_1 = m_1\omega^2x_1 \text{ for sinusoidal motion} \quad (1)$$

$$x = x_1 \sin\omega t \quad (2)$$

From continuity

$$\rho A_1V_1 = \rho A_2V_2 \; V_1 = x_1 \; V_2 = x_2 \quad (3)$$

$$x_1 = A_2/A_1x_2 = (d_2^2/d_1^2)x_2 = \alpha x_2 \quad (4)$$

$$P_1 = m_1\omega^2\alpha x_2/A_1 = m_1\omega^2x_2A_2/A_1 \quad (5)$$

$$x_2 = P_1A_1A_1/m_1\omega^2A_2 = P_1A_1/m_1\omega^2 \quad (6)$$

The total piston force is

$$F_2 = P_2A_2 = P_1A_1 + m_2\omega^2x_2 \quad (7)$$

Thus

$$P_2 = P_1 \pm m_2\omega^2x_2/A_2 \quad (8)$$

This analysis ignored all of the impedance effects and all of the perturbation pressure about the normal static pressure.

A Titan II, stage I turbopump was mounted to the missile engine frame as in a missile installation. The pump discharge lines, both fuel and oxidizer, were actual misssile hardware, including the thrust chamber valves. The pump hub was photographed through the camera port. The pump was driven by a gas generator with a separate pressure-fed propellant system using a bipropellant valve as the last valve.

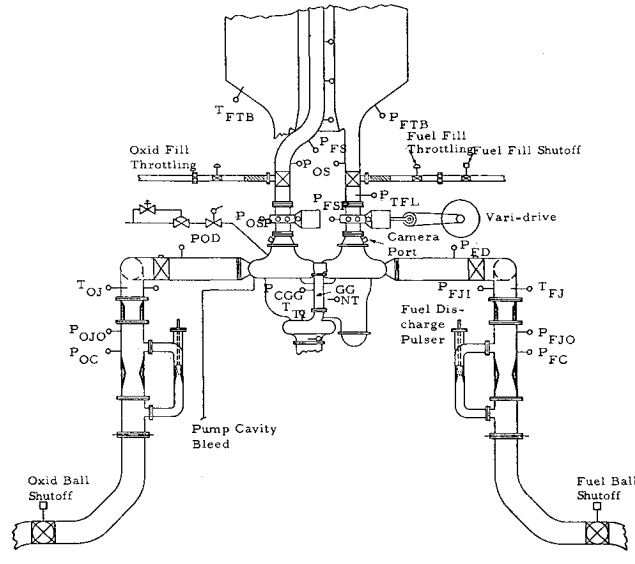

Fig. 1 Schematic of pogo test equipment.

Presented at the AIAA Space Simulation Testing Conference, Pasadena, Calif., November 16–18, 1964 (no preprint number; published in a bound volume of preprints of the meeting); revision received May 17, 1965.

* Group Engineer, Propulsion and Mechanical Department. Member AIAA.
† Engineer, Propulsion and Mechanical Department. Member AIAA.